



Detrended cross-correlation patterns between North Atlantic oscillation and precipitation

Hasan Tatli¹ · Şükran Sibel Menteş²

Received: 11 June 2018 / Accepted: 27 February 2019 / Published online: 15 March 2019
© Springer-Verlag GmbH Austria, part of Springer Nature 2019

Abstract

In this study, the long-range relationships between North Atlantic Oscillation (NAO) and precipitation data obtained from Climate Prediction Centre (CPC) Merged Analysis of Precipitation (CMAP) from 1979 to 2016 are investigated using Detrended Fluctuation Moving Average Cross-Correlation Analysis (DMCA). In the atmosphere, teleconnections through strong convective processes sporadically affect various climatic regimes in Europe, Mediterranean basin, North Africa, Middle East, and Caucasus. The NAO is one of the teleconnection processes and results in heavy rainfall in the Mediterranean basin during its negative phase while it gives rise to rain in Europe during its positive phase. The DMCA technique shows that the NAO fluctuation series exhibit different long-range cross-correlation coefficients, $\rho\text{DMCA}(s)$ with “s” being the moving average time window length, between the precipitation values and NAO. Large $\rho\text{DMCA}(s)$ coefficients with time window(s) larger than 12 months were obtained particularly over the Mediterranean basin, near the North Pole including northern Europe. Furthermore, the $\rho\text{DMCA}(s)$ coefficients were grouped into clusters using K-mean method to distinguish the similar patterns. The 1st cluster refers to the negative phase of the NAO indicating warm-rainy conditions and dry spells, which is especially evident in the Mediterranean basin. The 2nd cluster represents the long-range cross-correlation with respect to the positive phase of NAO and precipitation values, particularly for the Western and Northern Europe. Conversely, the 3rd cluster is evaluated as power law of long-range cross-correlations between the precipitation and NAO with respect to the different time scale processes.

Keywords DMCA · K-means · Mediterranean · NAO · Precipitation · Predictability

1 Introduction

Understanding complex processes in nature has become an active research area for researchers since the studies of Lorenz (1995), a meteorologist and pioneer of chaos theory. Because the natural systems are highly complex, it is important to identify dynamic properties, such as scale invariance, heavy skewness, non-linear correlations, non-stationarity and fractality in these processes.

Due to its simplicity, traditional Pearson correlation coefficient, ρ , analysis has become the most widely used method in

various fields including dynamical diagnosing and climate forecasting (Wilks 2011). However, ρ represents the linear correlation between two-time series assumed to be both stationary and Gaussian distributed. Since non-linear and non-stationary structures usually exist in natural systems (Lorenz 1995; Selvam 2017), ρ cannot be suitable to describe the cross-correlation between time series.

Most diverse complex systems consist of elements which are associated with each other in a commonly complex frame. The complexity of the interaction can be examined additionally based on, for example, the time history of each component as well as the time history of the other variables. These complex systems are generally characterized using “power-law of long-range cross-correlation”.

Peng et al. (1994) have suggested Detrended Fluctuation Analysis (DFA) for determining the long-range dependence in coding and non-coding of the DNA nucleotides sequence. This method is based on the random walk theory (Shlesinger et al. 1987), like the Hurst rescaled range analysis (Hurst 1951; Tatli 2015).

✉ Hasan Tatli
tatli@comu.edu.tr; tatli.hasan@gmail.com

¹ Department of Geography, Physical Geography Division, Faculty of Sciences and Arts, Çanakkale Onsekiz Mart University Terzioğlu Campus, 17020 Canakkale, Turkey

² Department of Meteorology, Istanbul Technical University, Maslak, 34469 Istanbul, Turkey

On the other hand, Detrended Cross-Correlation Analysis (DCCA; Zebende 2011) is an extended version of the DFA method. When compared to the classical correlation coefficient, the DCCA coefficient has an advantage such that it can be examined using different time scale, s . The performance of the DCCA has been systematically tested for the effect of stability. In addition, in the presence of non-stationarity, a wide range of applications has been derived to investigate the long-range cross-correlation of the signals (Podobnik et al. 2009; Vassoler and Zebende 2012; Zebende et al. 2013). The development of DCCA has led to invention/or/development of other alternative methods, such as detrended moving average cross-correlation analysis (DMCA; Jiang and Zhou 2011; Kristoufek 2014).

Many studies in climatology and meteorology, and other Earth Sciences in which the complex systems, occur address on such cross-interactions between different systems. For example, Ivanova and Ausloos (1999) applied the DFA method to microwave radiometer data for describing cloud breaking. These authors demonstrated that the liquid-water content in the Stratus cloud has a “long-range power-law correlation” over 2 h. Király and Jánosi (2005) analysed daily temperature anomaly data recorded in Australia and Hungary using the DFA technique. They found that the positive long-range asymptotic correlations can be as high as 5–10, and the generalized Hurst exponents for these places decreased with increasing distance from the Equator. Koscielny-Bunde et al. (2006) studied long-range temporal correlations and multifractal properties of long-river discharge records from 41 hydrological stations around the globe by employing the multifractal DFA (MFDFA) analysis. They found that at some transition times, usually around weeks, the daily runoffs were characterized by an asymptotic scaling factor, which indicates a slow power-law that uses runoff autocorrelation function, and changes from river to river. Zhang et al. (2008) applied MFDFA technique for scaling and multifractal properties of the hydrological processes of the Yangtze River basin in China. The authors determined different correlations for the upper, middle and lower streamlines of the Yangtze River basin. The discharge series of upper Yangtze River basin were characterized by a short memory or an anti-persistence, and the streamline of the lower Yangtze River basin was characterized by a long-memory or a persistence. Orun and Koçak (2009) applied the DFA method to obtain scaling exponent of daily mean temperature, maximum temperature, minimum temperature and temperature differences for 52 stations in Turkey. These researchers investigated the local changes of scaling exponents and their spatial distribution in Turkey and found four types of scaling exponents greater than 0.5, which is considered as long-range correlation. Guo et al. (2017) investigated the threshold of extreme precipitation events by the MFDFA technique in the mid-west of Jilin province located in North-East China. They concluded that the MFDFA method reveals the precipitation characteristics of the region, and they try to

find a relationship between internal precipitation for different time windows; therefore, the MFDFA could be an objective method to define the extreme precipitation threshold. Liu et al. (2016) suggested multifractal spectra analysis based on empirical mode decomposition approach and the DFA to measure the complexity in the monthly precipitation series. They concluded that precipitation series exhibit long-range correlation and are sensitive to changes in the initial values due to the long-term memory characteristics. Wang et al. (2016) have investigated the scaling features of wind speed time series by using the MFDFA. These authors suggested that by using the MFDFA of the wind speed time series, the segment length should be longer than 1 day, and the diel variation of wind should be maintained to avoid abnormal events.

The importance of the NAO in predicting climate has been further emphasized in the numerous studies in which the NAO was used to relate climate and weather resulting from the migrating surface pressure dipole over the North Atlantic region. The dominant atmospheric circulation variability mode of the NAO was shown to have a carrier role in winter climate fluctuations in a wide range of regions in Europe, Mediterranean, Middle East and North America (Hurrell 1995; Deser et al. 2017). For example, Beranová and Kyselý (2017) investigated the daily precipitation in the Czech Republic from 1961 to 2012 for examining the changes in seasonal precipitation indices, and their spatial patterns connection with temperature and atmospheric circulation. As reported in many studies, the NAO has negative correlations with precipitation series in the southern Europe and positive correlations in the northern Europe (Hurrell 1995; Ben-Gai et al. 2001; Turkes and Erlat 2003; Mariotti and Arkin 2007; Lopez-Moreno et al. 2011; Nada 2012; Delworth et al. 2016; Madrigal-González et al. 2017). Furthermore, Caldeira et al. (2007) studied the predictability of the NAO index using the DFA technique. They stated that the generalized Hurst exponent obtained from the DFA method for the annual series that were analysed show exhibits very little predictability of the NAO.

The organization of this article is as follows: a brief description of the NAO's characteristics of interaction with regional climate processes and a prospect on the hydro-meteorological applications are given in the next section. The dataset and procedures of the DCCA and the DMCA methods are presented in Sect. 3. The main results and a discussion are given in Sect. 4. Finally, the conclusions are drawn in Sect. 5.

2 A look on North Atlantic Oscillation

Due to the irregularities in the land-sea distribution in the Northern Hemisphere, the spatial distribution of spherical mean-pressure fields and related global wind systems do not form a zonal belt as in the Southern hemisphere, where the ocean areas cover large areas. In addition, generally, the semi-

continuous low and high-pressure centres outside the equatorial low-pressure zone are in an order. Near the middle latitudes, these climatic conditions are subject to seasonal and even shorter periodic changes, especially due to different heating of the land and sea surfaces, and therefore, prevailing winds in the middle latitudes are often very strong. The dynamic subtropical high-pressure systems (Pacific and Azores) centred at the eastern shores of the oceans approximately between 20 and 35° N latitudes tend to maintain their features throughout the year while comparing with the middle latitude systems. These high-pressure centres have major decisive influences on the climates of the great terrestrial areas located at their east regions.

In the Northern Hemisphere, the winter subtropical high-pressure systems are centred over the oceans due to spatial expanding and strengthening of the thermic high-pressures, Siberian and North American (Canadian/Greenland), which show a regional weakening due to strong cooling in large continental areas in the north. On the other hand, dynamic semi-continuous and cold low-pressure systems around 60° N latitude on the North Atlantic (Iceland) and North Pacific (Aleutian) effectively extend their influence on general flows over ocean between the southern 30–35° N latitudes. Therefore, there are strong precipitation and storms over areas where these pressure systems are effective. In summer months, due to heating of large terrestrial areas, cold-originated high-pressure centres become narrower and weaker and start to move towards the upper reaches of the polar regions replaced by thermic low-pressures. Here, a thermal low-pressure area is defined as it evolves to a difference in air pressure, which is achieved by a warming (insolation) or a cooling. A ground low or height low depends on the respective weather zones.

The warm subtropical anticyclones, centred on the eastern shores of oceans along subtropical latitudes, become stronger over oceans during summer, and they direct flows to the lands by expanding their influence. Due to seasonal cooling and warming processes in the North Hemisphere, latitudinal shifts in the developed wind systems (in the north–south direction) corresponding to semi-continuous pressure systems cause changes in seasonal weather conditions, especially in the middle latitudes. Near these latitudes, subtropical high pressures are effective in summer; a warm and dry climate is experienced in the southern Europe and Mediterranean basin regions. On the other hand, subpolar cyclones (extratropical cyclones) and those associated with frontal systems in winter cause strong precipitation and storms while they move to the southern latitudes.

Furthermore, during summer months, a thermic Asiatic monsoon in the central and southern Asia extends its influence area to the northern and western places. At the same time, Intertropical convergence zone (ITCZ) shifts to the northern of equator (South Asia) due to the warming in terrestrial areas. Accordingly, severe monsoon rains occur in the South and Central Asia due to the warm and humid air transporting to north regions over the ocean areas. Moreover, due to the warm

thermic Asian monsoon and dry and warm eastern and south-eastern flows are effective. These conditions cause to form the arid climates in the Arabia and in south-eastern parts of Turkey, located in the south-western Asia (Barry and Chorley 2003; Linacre and Geerts 1997; Turkes 2010).

The interactions of surface pressure patterns on the lands and oceans cause changes in climate variables such as temperature and precipitation. These changes are also related to large-scale oscillations due to general circulation of the atmosphere. The North Atlantic Oscillation is one of these large-scale atmospheric oscillations, particularly affects a wide-range area extending over northern regions of the America, Europe, Mediterranean and north-west Asia. The NAO controls large synoptic weather systems, and consequently, regional climate anomalies change regimes of temperature and precipitation (Hurrell 1995; Deser et al. 2017).

Rogers (1984) developed the NAO index for winter. The index is defined as the difference between the standardized winter surface pressure for Ponta Delgada station (the Azores) and that for Akureyri station (the Iceland), and it is defined as positive phase when the subtropical high-pressure value is higher than normal, the opposite-case is defined as negative phase.

The Azores High, also known as subtropical North Atlantic high (or Bermuda–Azores High), is a large subtropical semi-permanent centre of high atmospheric pressure, typically sited in the south of the Azores in the Atlantic Ocean. It is one the dipoles of the North Atlantic release, and the other pole is the Icelandic Low system, affecting wide regions of the North Africa and Southern Europe and, to a lesser extent, the weather and climate patterns of eastern North America. The aridity of the Sahara Desert and the summer drought of the Mediterranean basin are due to the large-scale collapse and sinking of the air in the system. The summer season is centred near Bermuda High and forms a south–west warm air flow towards the eastern coasts of the USA.

During the positive phase of NAO, warm and rainy weather conditions are experienced in regions near the high latitudes over the northern Atlantic and northern Europe, but in the south of Europe and the Mediterranean and south–west Asia, a cold and dry period prevails. In the negative phase of NAO, warm and rainy conditions prevail over the Mediterranean basin with contributions of the travelling cyclones corresponding to the Polar Jet flows (Stephenson et al. 2003; Li et al. 2011).

3 Data and methodology

3.1 Datasets

The rainfall data used in this study was obtained from the Climate Prediction Centre (CPC) Merged Analysis of Precipitation (CMAP; Xie and Arkin 1997) and are available

since 1979 to present. The CMAP is produced by a merging technique of combining multisatellite and rain gauge observations. It includes the Special Sensor Microwave/Imager (SSM/I), infrared-based Geostationary Operational Environmental Satellites (GOES) Precipitation Index (GPI) and Outgoing Longwave Radiation (OLR) Precipitation Index (OPI) and Microwave Sounding Units (MSU) data along with gauge information.

The monthly NAO index used in this study can be obtained from the following website: <http://www.cpc.ncep.noaa.gov/products/precip/CWlink/pna/norm.nao.monthly.b5001.current.ascii.table> (Climate Prediction Center, National Weather Service, NOAA).

3.2 Detrended cross-correlation analysis

The procedures of the DCCA method consist of five steps (Podobnik et al. 2009). Suppose that $x(t)$ and $y(t)$ are two-time series of length L . In the first step, their profiles (or integrated signals) are computed.

$$X_k = \sum_{i=1}^k x_i - \bar{x} \text{ and } Y_k = \sum_{i=1}^k y_i - \bar{y} \tag{1}$$

where $k = 1, 2, \dots, L$, and \bar{x} and \bar{y} represent the arithmetic means of the time series, respectively.

In the second step, each profile is divided into, $L_s = [L/s]$, non-overlapping segments of equal length “ s ”. Since the length L of the time profiles is often not a multiple of the time scale s , a residue may remain at the end of the profile. To take this part into account, the same procedure is repeated starting from the opposite site.

In the third step, a local trend is fitted by the least square sense for each of the N_s sections. Then, the covariance is determined for each segment as, $r = 1, \dots, L_s$.

$$f_r(s) = \frac{1}{s} \sum_{k=1}^s \left[X[(r-1)s + k] - \tilde{X}_r(k) \right] \times \left[Y[(r-1)s + k] - \tilde{Y}_r(k) \right] \tag{2}$$

where $\tilde{X}_r(k)$ and $\tilde{Y}_r(k)$ are the fitted polynomials in the related segments and r could be linear, quadratic, cubic, or higher order used in the fitting procedure.

In the fourth step, all segments are averaged to obtain q -th order of the DCCA.

$$F_{xy}(q, s) = \left\{ \frac{1}{Ls \sum_{r=1}^{N_s} [f_r(s)]^{q/2}} \right\}^{1/q} \tag{3}$$

for $q = 0$;

$$F_{xy}(0, s) = \exp \left[\frac{1}{2Ls} \sum_{r=1}^{N_s} \ln f_r(s) \right] \tag{4}$$

$F_{xy}(q, s)$ is dependent on time scale s for different values of q . For this study, the standard DCCA procedure was preferred by inserting the value of q equal to 2 in Eq. (3). The DFA method is a special case of the DCCA technique when $x(t) = y(t)$.

In the last step, the time scale behaviour of fluctuation functions is determined by fitting a log–log plot of $F_{xy}(q, s)$ versus s . The cross-correlation between $x(t)$ and $y(t)$ has a power law when the logarithms of $F_{xy}(q, s)$ and s jointly increase as seen in Fig. 1b.

The other method, so called the DMCA, F_{DMCA}^2 , is defined by He and Chen (2011) as in the following.

$$F_{DMCA}^2(s) = \frac{1}{L-s+1} \sum_{i=[s-\theta(s-1)]}^{[T-\theta(s-1)]-1} (X_k - \tilde{X}_{k,s}) (Y_k - \tilde{Y}_{k,s}) \tag{5}$$

where s is the window length of the moving average and θ is the moving-average type (forward, centred and backward for $\theta = 0, \theta = 0.5$ and $\theta = 1$, respectively). In this study, backward type was chosen. $\tilde{X}_{k,s}$ and $\tilde{Y}_{k,s}$ represent the specific moving averages with the window length s , at time step k . When this quantity is standardized by the DFAs, the DMCA cross-correlation coefficients are obtained as follows.

$$\rho_{DMCA}(s) = \frac{F_{DMCA}^2(s)}{F_{x,DMA}(s) \cdot F_{y,DMA}(s)} \tag{6}$$

where $F_{x,DMA}(s)$ and $F_{y,DMA}(s)$ are the detrended variances defined by

$$\left. \begin{aligned} F_{x,DMA}^2(s) &= \frac{1}{L-s+1} \sum_{i=[s-\theta(s-1)]}^{[T-\theta(s-1)]-1} (X_k - \tilde{X}_{k,s})^2 \\ F_{y,DMA}^2(s) &= \frac{1}{L-s+1} \sum_{i=[s-\theta(s-1)]}^{[T-\theta(s-1)]-1} (Y_k - \tilde{Y}_{k,s})^2 \end{aligned} \right\} \tag{7}$$

The DMCA cross-correlation coefficient has the same range as the standard correlation coefficient.

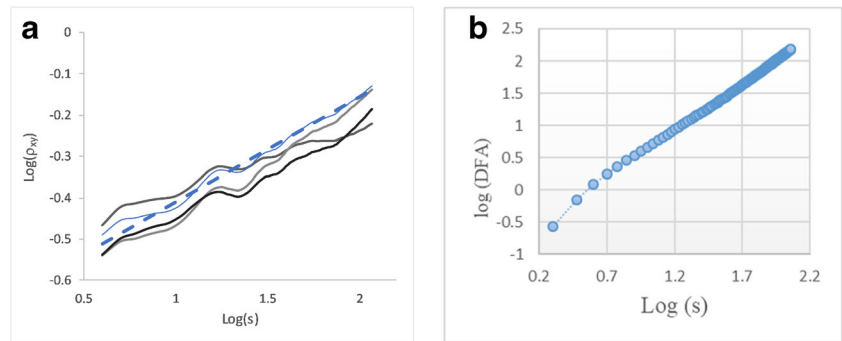
$$-1 \leq \rho_{DMCA}(s) \leq 1 \tag{8}$$

Power law of cross-correlations was ensured if the following scaling relationship is achieved.

$$\rho_{DMCA}(s) \propto s^{H_{xy}} \tag{9}$$

Here, the exponent, H_{xy} , is named the generalized Hurst exponent that designates power-law of the cross-correlations between the related time series. This exponent is determined by fitting a slope of the log–log states of the curves. For example, log–log states of the $\rho_{DMCA}(s)$ coefficients between the NAO and precipitation values at several grid points are shown in Fig. 1a. Similarly, the DFA fluctuations of the NAO index are shown in the Fig. 1b.

Fig. 1 Power-law dependence of the fluctuation functions on the time scale s (in months): cross-dependency between the NAO and different rainfall series. The dotted line represents the fitted curve log–log scale (a), and the slope of the line is the detrended fluctuations of the NAO (b)



If H_{xy} ranges between 0.5 and 1, there can be a predictability of the processes; otherwise, an inverse or a short-term correlation can be specified. However, if the H_{xy} is greater than 1, then, there will not be a fractal structure, and the negative H_{xy} indicates that a power law does not exist.

In this study, the DMCA cross-correlations were clustered in similar spatial groups to assess *long-range power law*. The K -mean algorithm clustering method was preferred for this study because of its easy applicability (Jain 2010; Turkes and Tatli 2011).

Based on the literature available in this field, a commonly accepted statistical test for the DMCA in the universal context has not yet been developed. Therefore, a significant critical value for the DMCA(s) correlation coefficients was found by generating 500 randomly distributed time series at each grid point. Since the average of the critical values was found to be in the range of [0.07–0.22], a critical value of 0.25 was selected, which just greater than 0.22. Our applied method is similar to the Monte Carlo approach, which is a method used in various fields (Tatli 2007; Wilks 2011).

4 Results and discussion

Figure 2 shows the statistically significant long-range cross-correlations with the generalized Hurst exponents between the NAO and precipitation series in the Ireland's north–west region of the ocean and west coasts of North Africa, Bulgaria, Romania, Poland and Eastern Europe including Latvia, central Anatolian plateau of Turkey, north–east Africa, Syria and Iraq.

In addition, the statistically significant correlations are observed in the west and north–west of the Britain Islands, in the north–west coasts and north–east Africa, in Portugal, in the east of Spain, in the Middle East, in the east of Europe, and Turkey's central Anatolian plateau corresponding to the positive or negative phases of the NAO values being related to the rainy or arid weather conditions. However, it is very interesting that there is no long-range significant correlation observed

in the Western and Central Europe except in the middle region of Italy.

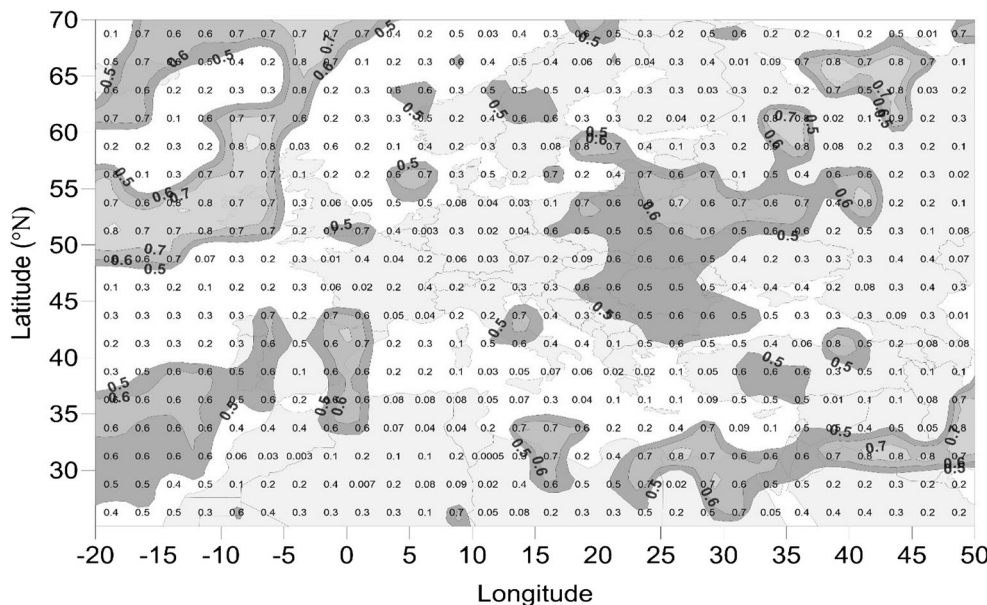
Here, using the DMCA method, power-law auto-correlations of monthly precipitation were also investigated. For this purpose, spatial distribution of the generalized Hurst exponents of the precipitation series is calculated as shown in Fig. 3. This figure shows the spatial distribution of generalized Hurst exponents obtained by the DFA approach. The generalized Hurst exponent indicates the long-term auto-regressive properties in the precipitation series that imply persistence (or predictability) (Tatli 2015). The Hurst exponents values which are greater than or equal 0.5 are seen in the regions of Iceland, the south–west British Islands, central Europe, south–western coast of Africa, North Africa, southern Europe, north–western Turkey, the Crimea, and in a wide area in the Middle East.

While the patterns given in Figs. 2 and 3 are surveyed together in the central and north Eastern Europe and Mediterranean basin, the effects of NAO are apparent in the areas where rainfall series have high persistence. On the other hand, in the regions where the Hurst exponents are smaller than 0.5 signify short or negative relationships.

The cross-correlation coefficients obtained by applying the DMCA method between the NAO and precipitation series are investigated for various time scales (s) as shown from Fig. 4. The time scale used in the study starts from 2 to 116 months. As seen in Fig. 4a, the significant DMCA cross-correlation coefficients calculated for 2-month period, $\rho_{DMCA}(2)$, are positive in the regions of Iceland, northern UK and Sweden. They explain the state of the NAO (positive or negative), and the NAO shows that it is particularly effective on the precipitation during its positive phase effectual precipitation (especially in the winter months).

The cycles (or time scales) of 3 and 6 months show similar patterns as obtained for the 2-month given in Fig. 4b, c. However, as time scale, “ s ” of the analysis increases, the DMCA positive correlation coefficients increase and indicate the spatial expansion of the regions influenced. The long-range cross-correlation is given in Fig. 4d for time scale of 12 months. The negative correlation coefficients are observed

Fig. 2 Spatial distribution of the generalized Hurst exponents computed between the NAO and precipitation series. The magnitude of the exponent indicates the long-term cross-correlation coefficient between the precipitation series and NAO

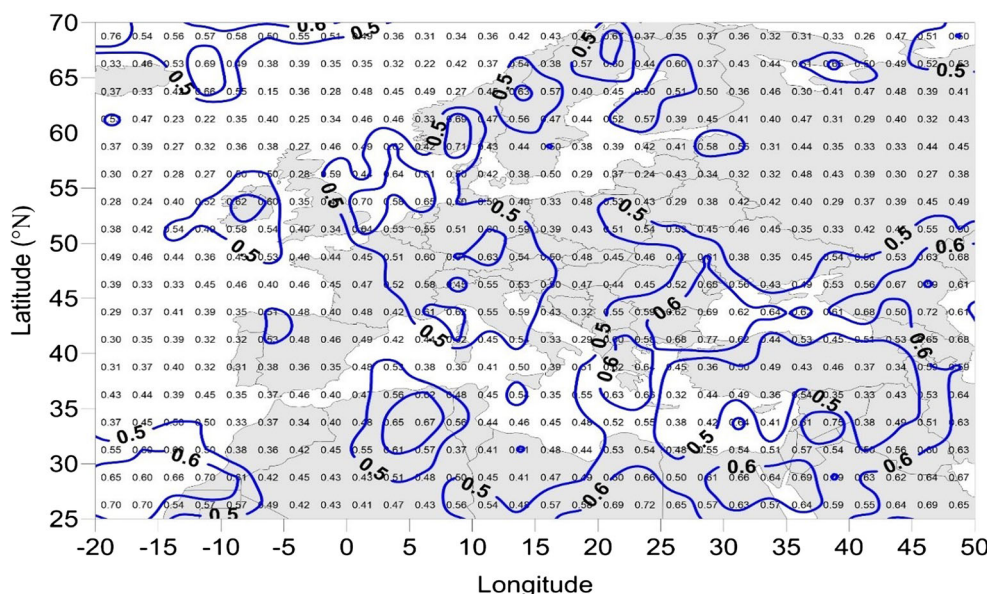


in the Eastern Europe, western Mediterranean and western coasts of Africa, while high positive correlation coefficients are influential in the northern regions. The coefficients less than 0.5 in this map imply negative or short-term relationships between the precipitation series and the NAO. Especially in winter months, while the NAO is in positive phase, the negative DMCA cross-correlation coefficients show relatively drought conditions, and contrarily, during the negative phase of the NAO, the positive DMCA cross-correlations mark the warm and rainy conditions. These conditions particularly demonstrate the effects of Icelandic low-pressure centre and the Mediterranean frontal cyclones associated with the polar front moving from North Atlantic regions to south during the

period of which the effect of the Azores high-pressure centre coincides and is weakened. Following the trajectory corresponding to south and south-eastern polar jet stream, there is an important contribution to this process. Additionally, the polar jet follows a trajectory along the higher latitudes during the positive-phase NAO.

The spatial distribution of the ρ DMCA (60) coefficients obtained for the cycles over 60 months (5 years) is given in Fig. 4e. According to this figure, the relationship between the NAO and precipitation series is more evident, and the increasing values of ρ DMCA (60) indicate the expanding zones of influence in Mediterranean, Eastern and Southern Europe. Furthermore, the positive coefficients are common over the

Fig. 3 Generalized Hurst exponents computed by the DFA method for the precipitation series. It represents the long-range auto-correlation



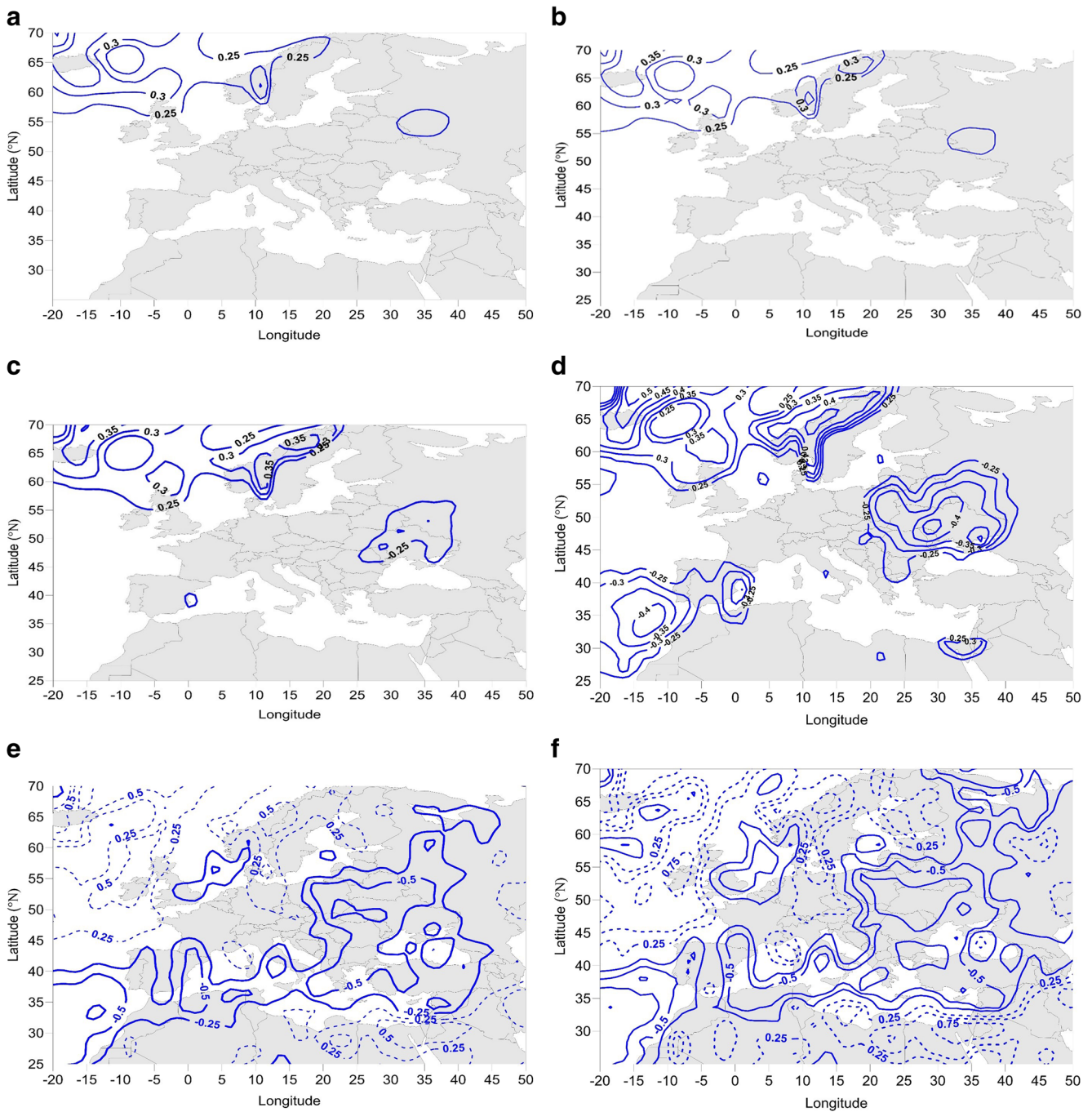


Fig. 4 Distribution of the long-range cross-correlation analysis (DMCA) between the NAO and precipitation series for different time scales. **a** $s = \text{cycles}/2$ months. **b** $s = \text{cycles}/3$ months. **c** $s = \text{cycles}/6$ months. **d** $s = \text{cycles}/12$ months. **e** $s = \text{cycles}/60$ months. **f** $s = \text{cycles}/115$ months

western borders of Europe and Central Europe, and magnitude of those coefficients on Britain reaches as high as 0.75 (Fig. 4e, f). The Icelandic low-pressure centre deepens as the Azores high pressure strengthens due to the polar front associated with this low pressure, travelling eastward through the North Atlantic, Northern and Central Europe experiences rainy period. Accompanying, due to the Azores anticyclone strengthened in Southern Europe, movement of the western flows and frontal systems following these flows are prevented

towards the Mediterranean. Consequently, dry weather conditions often occur in Eastern and Southern Europe, north-western Africa and Turkey.

In the negative phase of NAO, the process is reversed. Depending on the movement of western currents through to the Atlantic Ocean and Mediterranean fronts along southwest–northeast direction associated with the movement cyclones, warm and rainy air conditions occur during the spatial path of these cyclones.

The DMCA cross-correlation patterns for the 5-year or longer time scales between the rainfall series and NAO are shown in Fig. 4e, f. In these maps, some important notes can be highlighted in Central and East Africa: (1) subpatterns in this region behave very different in southern Europe compared to the Mediterranean regions. (2) During the negative phase of the NAO, the fronts cannot be so close to these latitudes because of their trajectories originating from the Mediterranean frontal regions in NW and NE directions, resulting in warm and dry weather conditions.

Clustering of the $\rho\text{DMCA}(s)$ coefficients by using K -mean method show three major groups as given in Fig. 5. The first cluster given in Fig. 5a represents the distribution patterns related to the negative phase of the NAO, and these patterns denote the long-range negative cross-correlation coefficients between the NAO and precipitation data, which is especially evident in the Mediterranean basin.

On the other hand, the second cluster given in Fig. 5b indicates the situations where the $\rho\text{DMCA}(s)$ coefficients are very weak between the NAO and precipitation values, and it represents the positive phase of NAO, particularly for the Western and Northern Europe. The third cluster given in Fig. 5c illustrates the group's the long-range correlations between the NAO and precipitation series; it might be evaluated as the power law of long-range cross-correlations between the precipitation and NAO with respect to the different time scale processes without taking account the positive or negative phases of the NAO.

5 Conclusions

The DMCA technique is a generalization of the DFA approach based on detrended covariance to illustrate the cross-correlation between two different non-linear and non-stationary variables. In this background, we applied the DMCA method to explore the long-range power law of the cross-correlations between the NAO and precipitation series.

The analysis results show the long-range cross-correlations between the precipitation series and the NAO over a large area between $25\text{--}70^\circ$ N latitudes and $20\text{ W--}70^\circ$ E longitudes spreading in Europe, the Mediterranean basin and the north-west Asia and North Africa. Our main findings are summarized as follows.

In the first step, we have shown how the long-range auto-correlation of the precipitation sequences changes in different time scales (represented by the symbol s) by the MDFA approach.

In the second step, the long-range cross-correlation coefficients, $\rho\text{DMCA}(s)$, were obtained by the DMCA method. We have shown that the spatial distribution of the magnitude and sign of the $\rho\text{DMCA}(s)$ obtained at different time scales may be related to the positive and negative phases of the NAO.

Specifically, the significant cross-correlation coefficients of $\rho\text{DMCA}(2)$ are positive in the regions covering Iceland, north England and Sweden. These patterns explain the precipitation processes in winter months associated with the NAO, as the low-pressure centre in Iceland over the North Atlantic cause influential precipitation when the NAO is in its positive phase.

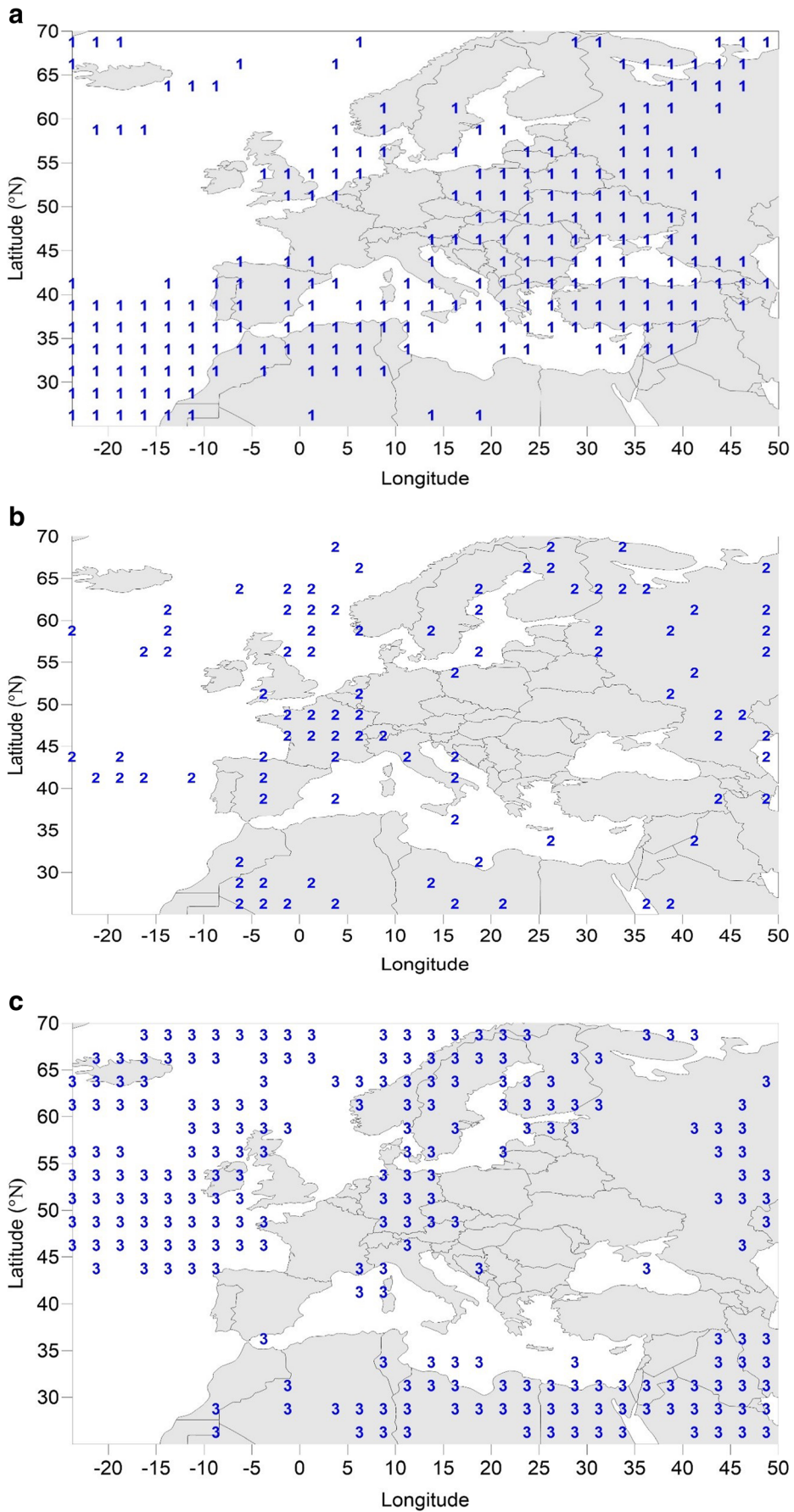
Furthermore, as the time scale s increases, the magnitude of $\rho\text{DMCA}(s)$ also increases, and the geographical domain that was affected also expands. In addition, while the negative cross-correlation coefficients, $\rho\text{DMCA}(12)$, are observed on the western coasts of Eastern Europe, the western Mediterranean and Africa, the high positive cross-correlation coefficients are obtained in the northern regions. This last result may imply the negative or short-term relationship between the precipitation values and NAO.

The magnitude of $\rho\text{DMCA}(60)$ coefficients increases towards the borders of western and central Europe, and these coefficients in the UK reach up to 0.75. The large correlation coefficients observed here indicate the long-term strong cross-relationship (or predictability) between the precipitation and the NAO.

As a result, the preliminary analysis results demonstrate that long-range cross-correlations between the NAO and precipitation series on the orders of 12 month, and longer time were found to be much more significant than those of the short-time periods. Contrary to the studies based on the classical correlation method, while the classical correlation approach shows a very short-term relationship, the detrended (and also cross) fluctuation analysis method is capable of determining the long-term relationship in a selected arbitrary time scale, s .

In addition, when the cross-correlation coefficients, $\rho\text{DMCA}(s)$, are clustered for all time scales (s), three separate clusters were obtained. The first cluster represents pattern that corresponds to the negative-phase state of the NAO. This cluster is a group that shows the regions where the negative cross-correlation, $\rho\text{DMCA}(s)$, was observed. It was demonstrated that these regions where the negative cross-correlations were seen remain under the influence of the negative phase of the NAO resulting in warm and rainy periods, and dry spell if the NAO is in its positive phase. The second cluster represents the situations where the $\rho\text{DMCA}(s)$ coefficients are weak, i.e. the patterns in these areas are the regions where the effect of NAO is not very strong. The third cluster represents the features of both positive and negative phases, or a group of the rainfall sequences, which are strongly correlated with the NAO. In other words, cluster 3 is the group that presents the long-range $\rho\text{DMCA}(s)$ coefficients between the NAO and precipitation series. During the positive phase of the NAO,

Fig. 5 K -mean clustering of the DMCA cross-correlation coefficients between precipitation series and NAO for all cycles (or time scales) from 2 to 115 months. **a** First cluster. **b** Second cluster. **c** Third cluster



these zones are warm and rainy, but cold and dry meteorological conditions are usually experienced during the negative phase.

The long-range cross-correlations between the NAO and precipitation series were found in a wide range of area including entire Europe, the Mediterranean, North Africa, Middle East and Caucasus. Therefore, considering the large size of the study area, it is known that the Arctic and Mediterranean oscillations (Higgins et al. 2002; Palutikof et al. 1996; Conte et al. 1989) give rise to influential hydro-meteorological conditions in some subregions. It is expected that the impacts of these oscillations on the precipitation patterns will be a research topic with the method discussed in this study.

References

- Barry RG, Chorley RJ (2003) Atmosphere, weather and climate, Eighth edn. Routledge, London
- Ben-Gai T, Bitan A, Manes A, Alpert P, Kushnir Y (2001) Temperature and surface pressure anomalies in Israel and the North Atlantic Oscillation. *Theor Appl Climatol* 69:171–177 <https://doi.org/10.1007/s007040170023>
- Beranová R, Kyselý J (2017) Trends of precipitation characteristics in the Czech Republic over 1961–2012, their spatial patterns and links to temperature and the North Atlantic Oscillation. *Int J Climatol* 38:e596–e606. <https://doi.org/10.1002/joc.5392> (in Press)
- Caldeira R, Fernández I, Pacheco JM (2007) On NAO's predictability through the DFA method. *Meteorog Atmos Phys* 96:221–227
- Conte M, Giuffrida A, Tedesco S (1989) The Mediterranean oscillation. Impact on precipitation and hydrology in Italy climate water. Publications of the Academy of Finland, Helsinki
- Delworth TL, Zeng F, Vecchi GA, Yang X, Zhang L, Zhang R (2016) The North Atlantic oscillation as a driver of rapid climate change in the Northern Hemisphere. *Nat Geosci* 9:509–512 <https://doi.org/10.1038/ngeo2738>
- Deser C, Hurrell JW, Phillips AS (2017) The role of the North Atlantic oscillation in European climate projections. *Clim Dyn* 49:3141–3157
- Guo E, Zhang J, Si H, Dong Z, Cao T, Lan W (2017) Temporal and spatial characteristics of extreme precipitation events in the Midwest of Jilin Province based on multifractal detrended fluctuation analysis method and copula functions. *Theor Appl Climatol* 130:597–607
- He LY, Chen SP (2011) A new approach to quantify power-law cross-correlation and its application to commodity markets. *Physica A* 390:3806–3814
- Higgins RW, Leetmaa A, Kousky VE (2002) Relationships between climate variability and winter temperature extremes in the United States. *J Clim* 15:1555–1572
- Hurrell JW (1995) Decadal trends in the North Atlantic oscillation: regional temperatures and precipitation. *Science* 269:676–679
- Hurst HE (1951) Long term storage capacity of reservoirs. *ASCE Transactions* 116:770–808
- Ivanova K, Ausloos M (1999) Application of the detrended fluctuation analysis (DFA) method for describing cloud breaking. *Physica A* 274:349–354
- Jain AK (2010) Data clustering: 50 years beyond K-means. *Pattern Recogn Lett* 31:651–666
- Jiang ZQ, Zhou WX (2011) Multifractal detrending moving-average cross-correlation analysis. *Phys Rev E* 84(1):016106
- Király A, Jánosi IM (2005) Detrended fluctuation analysis of daily temperature records: geographic dependence over Australia. *Meteorog Atmos Phys* 88:119–128
- Koscielny-Bunde E, Kantelhardt JW, Braun P, Bunde A, Havlin S (2006) Long-term persistence and multifractality of river runoff records: detrended fluctuation studies. *J Hydrol* 322:120–137
- Kristoufek L (2014) Detrending moving-average cross-correlation coefficient: measuring cross-correlations between non-stationary series. *Physica A* 406:169–175
- Li W, Li L, Fu R, Deng Y, Wang H (2011) Changes to the North Atlantic subtropical high and its role in the intensification of summer rainfall variability in the southeastern United States. *J Clim* 24:1499–1506
- Linacre E, Geerts B (1997) *Climates and weather explained*. Routledge, London
- Liu D, Luo M, Fu Q, Zhang Y, Imran KM, Zhao D, Li T, Abrar FM (2016) Precipitation complexity measurement using multifractal spectra empirical mode decomposition detrended fluctuation analysis. *Water Resour Manag* 30:505–522
- Lopez-Moreno JJ, Vicente-Serrano SM, Moran-Tejeda E, Lorenzo-Lacruz J, Kenawy A, Beniston M (2011) Effects of the North Atlantic Oscillation (NAO) on combined temperature and precipitation winter modes in the Mediterranean mountains: observed relationships and projections for the 21st century. *Glob Planet Chang* 77:62–76 <https://doi.org/10.1016/j.gloplacha.2011.03.003>
- Lorenz EN (1995) *The essence of Chaos*. University of Washington Press, Seattle
- Madrigal-González J, Ballesteros-Cánovas JA, Herrero A, Ruiz-Benito P, Stoffel M, Lucas-Borja ME, Zavala MA (2017) Forest productivity in southwestern Europe is controlled by coupled North Atlantic and Atlantic multidecadal oscillations. *Nat Commun* 8:2222. <https://doi.org/10.1038/s41467-017-02319-0>
- Mariotti A, Arkin P (2007) The North Atlantic oscillation and oceanic precipitation variability. *Clim Dyn* 28:35–51
- Nada PB (2012) The impact of arctic and North Atlantic oscillation on temperature and precipitation anomalies in Serbia. *Geogr Pannonica* 16:44–55
- Orun M, Koçak K (2009) Application of detrended fluctuation analysis to temperature data from Turkey. *Int J Climatol* 29:2130–2136
- Palutikof JP, Conte M, Casimiro Mendes J, Goodess CM, Espirito Santo F (1996) Climate and climate change. In: Brandt CJ, Thornes JB (eds) *Mediterranean desertification and land use*. Wiley, London
- Peng CK, Buldyrev SV, Havlin S, Simons M, Stanley HE, Goldberger AL (1994) Mosaic organization of DNA nucleotides. *Phys Rev E* 49:1685–1689
- Podobnik B, Horvatic D, Petersen AM, Stanley HE (2009) Cross-correlations between volume change and price change. *P Natl Acad Sci* 106:22079–22084
- Rogers JC (1984) The association between the North Atlantic Oscillation and the Southern Oscillation in the northern hemisphere. *Mon Weather Rev* 112:1999–2015
- Selvam AM (2017) Nonlinear dynamics and chaos: applications in meteorology and atmospheric physics. In: *Self-organized criticality and predictability in atmospheric flows: the quantum world of clouds and rain*. Springer Atmospheric Sciences, Cham, pp 1–40
- Shlesinger MF, West BJ, Klafter J (1987) Lévy dynamics of enhanced diffusion: application to turbulence. *Phys Rev Lett* 58:1100–1103
- Stephenson DB, Wanner H, Brönnimann S, Luterbacher J (2003) The history of scientific research on the North Atlantic Oscillation. In: Hurrell JW, Kushnir Y, Ottersen G, Visbeck M (eds) *The North Atlantic Oscillation: climatic significance and environmental impact*. American Geophysical Union, Washington, DC, pp 37–50. <https://doi.org/10.1029/134GM02>

- Tatli H (2007) Synchronization between the North Sea–Caspian pattern (NCP) and surface air temperatures in NCEP. *Int J Climatol* 27: 1171–1187
- Tatli H (2015) Detecting persistence of meteorological drought via the Hurst exponent. *Meteorol Appl* 22:763–769
- Turkes M (2010) *Climatology and meteorology*. Kriter Publisher, Istanbul in Turkish
- Turkes M, Erlat E (2003) Precipitation changes and variability in Turkey linked to the North Atlantic Oscillation during the period 1930–2000. *Int J Climatol* 23:1771–1796
- Turkes M, Tatli H (2011) Use of the spectral clustering to determine coherent precipitation regions in Turkey for the period 1929–2007. *Int J Climatol* 31:2055–2067
- Vassoler RT, Zebende GF (2012) DCCA cross-correlation coefficient apply in time series of air temperature and air relative humidity. *Physica A* 391:2438–2443
- Wang X, Mei Y, Li W, Kong Y, Cong X (2016) Influence of sub-daily variation on multi-fractal detrended fluctuation analysis of wind speed time series. *PLoS One* 11:e0146284
- Wilks DS (2011) *Statistical methods in the atmospheric sciences*. Academic Press, Cambridge
- Xie P, Arkin PA (1997) Global precipitation: a 17-year monthly analysis based on gauge observations, satellite estimates, and numerical model outputs. *B Am Meteorol Soc* 78:2539–2558
- Zebende GF (2011) DCCA cross-correlation coefficient: quantifying level of cross-correlation. *Physica A* 390:614–618
- Zebende GF, da Silva MF, Filho AM (2013) DCCA cross-correlation coefficient differentiation: theoretical and practical approaches. *Physica A* 392:1756–1761
- Zhang Q, Xu CY, Chen YD, Yu Z (2008) Multifractal detrended fluctuation analysis of streamflow series of the Yangtze River basin, China. *Hydrol Process* 22:4997–5003

Publisher's note Springer Nature remains neutral with regard to jurisdictional claims in published maps and institutional affiliations.